Temperature-dependent structural stability and optical properties of ultrathin Hf–Al–O films grown by facing-target reactive sputtering

G. He,[a] L. D. Zhang, G. W. Meng, G. H. Li, Q. Fang, and J. P. Zhang
Key Laboratory of Materials Physics, Anhui Key Laboratory of Nanomaterials and Nanostructure, Institute of Solid State Physics, Chinese Academy of Sciences, Hefei 230031, China

(Received 3 July 2007; accepted 9 September 2007; published online 1 November 2007)

The structural stability and optical properties of ultrathin $HfAlO_x$ films grown by facing-target reactive sputtering, depending on the postannealing temperature, have been determined via x-ray photoelectron spectroscopy and spectroscopic ellipsometry (SE). By virtue of the chemical shifts of Hf4f, Al2p, and Si2p core-level spectra, it has been found that the structural stability of $HfAlO_x$/Si system sustains up to 800 °C. However, the breaking of the Hf–Al–O bond and the phase separation take place drastically at the annealing temperature of 900 °C. In particular, the information of an interfacial Si–O–Si bond as the dominant reaction during the postannealing treatment has been observed, confirmed by Fourier transform infrared spectroscopy. Analysis by SE, based on the Tauc-Lorentz model, has indicated that increase in the refractive index and reduction in thickness has been observed as a function of annealing temperature, originating from the annealing-induced higher packing density. The change of the complex dielectric functions and bandgap E_g correlated with the annealing temperature are discussed in detail. © *2007 American Institute of Physics*.
[DOI: 10.1063/1.2802994]

I. INTRODUCTION

With the further downscaling of complementary metal-oxide-semiconductor field effect transistors (MOSFETs), conventional SiO_2 is approaching the fundamental limits where SiO_2 loses insulator properties due to tunneling current. As an alternative, high-k gate dielectric materials are proposed to replace SiO_2 gate oxides, in which higher dielectric constant allows the thicker physical thickness of gate oxides to suppress the leakage current.[1–3] Among various materials, HfO_2 has been considered to be one of the most promising dielectrics due to its considerably large energy bandgap, high dielectric constant, and compatibility with conventional complementary metal-oxide-semiconductor (CMOS) processes because of the superior thermodynamic stability.[4–7] However, HfO_2 films tend to crystallize at relatively low temperatures (500 °C), which causes larger grain-boundary leakage current.[8–10] More importantly, HfO_2 is a poor barrier to oxygen diffusion.[11,12] Annealing in an oxygen-rich ambient will lead to fast diffusion of oxygen through the HfO_2, causing the growth of uncontrolled low-k interfacial layers (either SiO_x or SiO_x-containing layer).[11] The uncontrolled low-k layer poses a serious limitation to further scaling of the equivalent oxide thickness for HfO_2 gate dielectrics.[13,14]

Currently, several research groups have investigated that alloying HfO_2 with Al results in the significant improvement in electric properties as well as in crystallinity.[15–17] Furthermore, due to their reasonable k value and the band offset value to Si, hafnium aluminates are regarded as a promising candidate for high-k gate dielectrics application.[18–20] Recently, two main processing techniques, atomic layer deposition (ALD) and metal organic chemical vapor deposition (MOCVD), have been pursued to deposit high-k $HfAlO_x$ films.[21,22] Both methods require complicated systems and operate at high temperatures, which accelerates the formation of interfacial SiO_2 layers and reduces the effective dielectric constant of the $HfAlO_x$ films. Additionally, the existence of residual impurities in the deposited film by ALD or MOCVD due to the use of precursor is unfavorable to the quality of high-k gate oxide.[23]

Although there have been reports on the $HfAlO_x$ films, most studies have been focused on the dielectric and optoelectronic applications based on its superior electrical properties. Metal-insulator-metal (MIM) capacitor with atomic-layer-deposited $HfAlO_x$ films on Si substrate has been demonstrated excellent electrical performance, especially extremely low leakage current.[19] Metal-oxide-semiconductor-metal (MOSM) capacitor with low temperature evaporated $HfAlO_x$ films thinner than 6 nm shows improved dielectric properties and breakdown electrical field.[15] Metal-ferroelectric-insulator-semiconductor field effect transistors (MFISFET) with long memory retention, based on $HfAlO_x$ insulator layer thinner than 10 nm, have been fabricated.[24,25] In spite of this application, by now, temperature-dependent interfacial structure and optical properties of $HfAlO_x$ have not been thoroughly investigated. In this letter, we focus on the characteristics of $HfAlO_x$ films on Si grown by facing-target reactive sputtering at room temperature. We have investigated the change of the chemical bonding states of the films as a function of annealing temperature using x-ray photoelectron spectroscopy (XPS) measurement. Spectroscopic ellipsometry (SE), a nondestructive technique for the determination of the optical properties of films, has been employed to investigate the optical characteristics of $HfAlO_x$ films. By spectroscopic spectra analysis based on the accu-

[a]Author to whom correspondence should be addressed. Electronic mail: ganghe01@yahoo.com.cn

 © 2007 American Institute of Physics

Downloaded 23 Jun 2010 to 61.190.88.137. Redistribution subject to AIP license or copyright; see http://jap.aip.org/jap/copyright.jsp

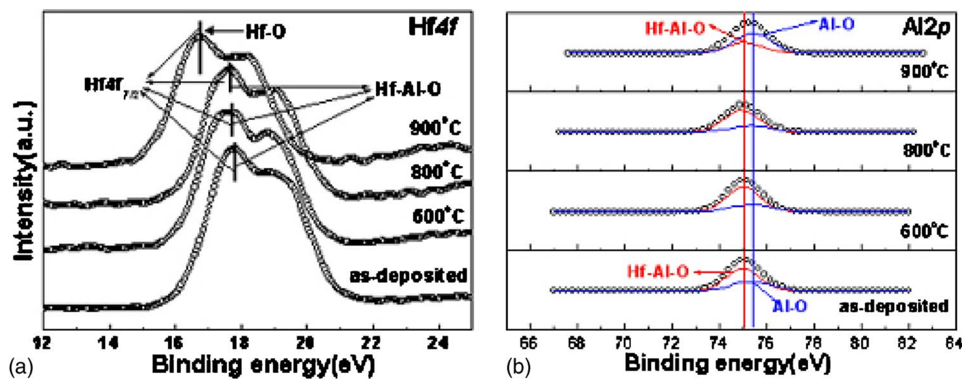

FIG. 1. (Color online) XPS spectra of Hf 4f (a) Al 2p (b) core levels for $HfAlO_x$ films as a function of annealing temperature.

rately parametrized Taul-Lorentz dispersion relation for the $HfAlO_x$ films,[26–28] the optical properties of the $HfAlO_x$ films correlated with annealing temperatures have been obtained. Meanwhile, analysis of the interfacial structure of $HfAlO_x$/Si as a function of annealing temperature is also carried out by Fourier transform infrared spectroscopy (FTIR).

II. EXPERIMENTAL DETAILS

Ultrathin $HfAlO_x$ films (~7 nm) were grown on n-Si (100) substrates by radio frequency facing-target reactive sputtering of Hf and Al target with purity of 99.99% at room temperature. Prior to growing the mixed oxide film, to remove organic and metallic impurities on the wafers, the n-type Si (100) substrates with a resistivity of 4–12 Ω cm were precleaned by a standard Radio Corporation of American (RCA) processing.[29] The intertarget distance and target-to-substrate distance are 80 and 70 mm, respectively. The sputtering was performed under a mixture of Ar and O_2 ambient supplied as working and reactive gases using independent mass flow controllers. The system was pumped to 2.5 $\times 10^{-5}$ Pa before Ar and O_2 gases were introduced. During sputtering, the sputtering powers for the Hf and Al target were kept at 100 and 80 W, respectively. The flow rates of Ar and O_2 gases were held at 17 and 3 SCCM (SCCM denotes cubic centimeter per minute at STP), respectively. All the films were submitted to thermal annealing in N_2 from 600 to 900 °C for 5 min. In order to assess changes in thermal stability of the film related with annealing temperature, the chemical bonding states of the targeted $HfAlO_x$ films have been investigated by *ex situ* XPS (ESCALAB MK2) system, equipped with a Mg Kα radiation source (1253.6 eV) and hemispherical analyzer with a pass energy of 20 eV. The collected data were corrected for charging effect-induced peak shifts using the binding energy of adventitious carbon C 1s peak (284.6 eV). An *ex situ* phase modulated spectroscopic ellipsometry (UVISEL Jobin-Yvon) measurement was performed with a spectral range of 0.75–6.5 eV in steps of 50 meV at room temperature. For interpreting the measured pseudodielectric function, a four-layer-structured optical model consisting of Si substrates (the optical constant taken from an reference c-Si film[30]), a SiO_2 interfacial layer formed at the $HfAlO_x$/Si interface (the optical constant taken from Ref. 31), a bottom bulk $HfAlO_x$ layer, and the surface rough layer consisting of 50% voids and 50% of the $HfAlO_x$ films, modeled by an effective medium approximation applying the Bruggeman formalism,[32] has been constructed to extract the optical functions of the as-deposited and annealed $HfAlO_x$ films. Analyses of the interfacial layer formed at the $HfAlO_x$/Si interface in relation to annealing temperature are performed by using Fourier transform infrared spectroscopy (Nicolet Magna-IR750).

III. RESULTS AND DISCUSSION

A. XPS characterization

Figure 1 shows the XPS spectra for Hf4f, Al2p, and Si2p core levels as a function of annealing temperature. From Hf4f core-level spectra shown in Fig. 1(a), it is observed that the Hf4$f_{7/2}$ peak at 17.8 eV for the as deposited, separated 1.4 eV from the Hf4$f_{5/2}$ peak at 19.2 eV, may due to the formation of Hf–Al–O bonds.[33] Compared with our reported Hf4f peaks (16.9 and 18.2 eV) for HfO_2,[10] there is a 0.8 eV shift of the Hf4$f_{7/2}$ peak toward a higher binding energy but lower than that of $HfSiO_x$, indicating the $HfAlO_x$ is predominant in the as-deposited films, and a small amount of $HfAl_xSi_yO_z$ and some remnants of HfO_2 were formed. This shift is likely due to the increased contribution of electron density to the Al–O bond in the Hf–Al–O compared with the electron density from Hf to oxygen, which is consistent with the relative electron negativity difference between Hf, Al, and O (1.30, 1.60, and 3.44 on the Pauling scale, respectively). The existence of $HfAl_xSi_yO_z$ means that during the formation processes of high-k dielectric on Si substrate, an interface layer consisting of silicates is unavoidable. However, the silicate formation itself was well suppressed in the $HfAlO_x$ film. According to the reported binding energy values for the Hf–Si bond, it should be noted that no deleterious Hf–Si bond formation is detected, it is an encouraging result. For the annealed samples from 600 to 800 °C, the change in the peak position and component has not been observed. After annealing at 900 °C, it can be noted that there is an apparent shift of Hf4f peaks toward lower binding energy, which can be attributed to the phase separation of Hf–Al–O into HfO_2 and Al_2O_3. For the as-deposited sample, the Al2p spectra are deconvoluted into two peaks by nonlinear Gaussian lineshapes, corresponding to Hf–Al–O and Al_2O_3. Compared to the binding energy of Al2p core level of pure amorphous Al_2O_3 thin film, peak 1 shows a slight shift toward lower binding energy, which can assigned to the formation of Hf–Al–O. This observation is in agreement with the conclusion confirmed by Zhu *et al.*[34]

Downloaded 23 Jun 2010 to 61.190.88.137. Redistribution subject to AIP license or copyright; see http://jap.aip.org/jap/copyright.jsp

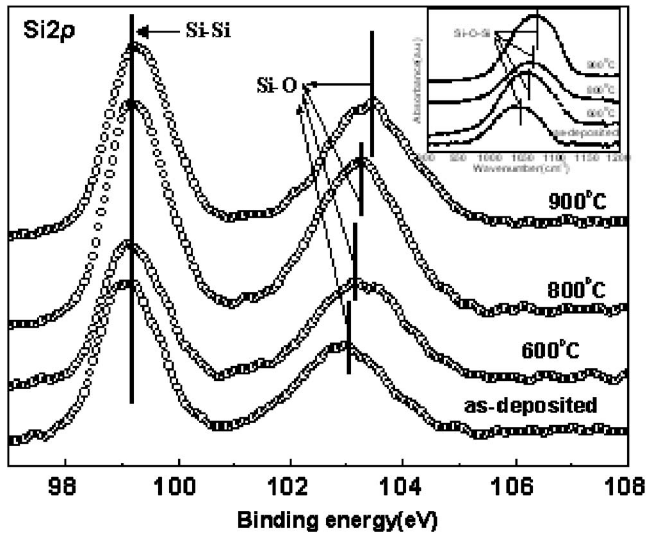

FIG. 2. XPS spectra of Si2*p* core levels for $HfAlO_x$ films deposited at room temperature and annealed in ambient of N_2 at 600, 800, and 900 °C, respectively. Inset in (c) shows the FTIR spectra of the as-deposited and annealed samples at different temperatures.

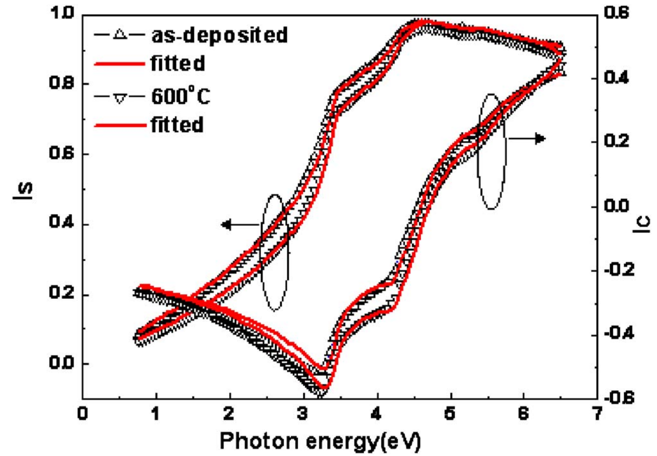

FIG. 3. (Color online) The experimental and fitted spectroscopic ellipsometric data for the as-deposited and annealed samples at 600 °C.

During annealing from 600 to 800 °C, it has been also found that there is no obvious change in the peak positions and intensity. After annealing at 900 °C, the peak intensity contributed to Al_2O_3 (75.3 eV) increases, while the peak intensity corresponding to Hf–Al–O component decreases abruptly, due to the phase separation of Hf–Al–O into HfO_2 and Al_2O_3. According to the report from Jin *et al.*, annealing the $HfAlO_x$ thin film up to 950 °C will accelerate the separation of $HfAlO_x$ and the formation of HfSi at the interface region.[33] Thus, more work of the evolution of the interfacial structure related with postannealing temperature beyond 900 °C is underway.

The information of the interfacial chemical bonding states correlated with postannealing temperature can also be obtained from the Si 2*p* core-level spectra. The Si2*p* core-level XPS spectra for the as-deposited and annealed samples are shown in Fig. 2. From Si 2p core-level spectra shown in Fig. 2, it can be seen that the peak located at 99.3 eV is attributed to Si–Si bonds from Si substrates and the peak at 103.0 eV relates to the Si–O bonds from the interfacial layer near the Si surface. Compared with thermal oxidized SiO_2, the Si2*p* peak, corresponding to SiO_2, shifts toward lower binding energy, from 103.5 to 103.1 eV. This can be due to the reaction of the initial remanent SiO_x layer on the Si substrate with the deposited films and the formation of an interfacial suboxide $SiO_{x<2}$.[35] From Fig. 2, it is apparent that the interfacial layer exists for the as-deposited and annealed samples, independent of the annealing temperature, which is in agreement with the report from Yu *et al.*[36] With the increase of the annealing temperature, it is notable that the chemical shift of the peaks with respect to $SiO_{x<2}$ moves toward higher binding energy. We contribute the shift to the charging phenomenon within a pure SiO_2 and the dominant Si–O–Si bond formation reaction during oxidation, which is in agreement with the conclusion of Iwata *et al.*[37] According to our previous report, the evolution of the interfacial component related with postannealing temperature can be obtained from FTIR analysis.[38] Shown in inset of Fig. 2 an absorption peak located at 1045 cm^{-1} has been observed for the as-deposited sample, which is due to the Si–O stretching vibration in the interfacial layer. Annealing brings about a slight shift of the vibration peak position of Si–O bonds toward higher wavenumber, close to the value of Si–O stretching vibration in bulk SiO_2 at 1075 cm^{-1}. This result indicates that postannealing can convert suboxide (SiO_x) at the interface into stoichiometric SiO_2, which can help to improve the interfacial quality. According to the results confirmed by XPS and FTIR, it has been observed that the intensity of Si–O bonds has not demonstrated apparent change with the increase of annealing temperature, indicating that the interface reaction was well suppressed in the Hf–Al mixed oxide film. Therefore, it can be concluded that the ability to block oxygen diffusion through HfO_2 films is greatly enhanced by the incorporating of Al_2O_3.

B. Optical characterization

Despite their potential dielectric and optoelectronic applications, the optical properties of $HfAlO_x$ thin films have not been thoroughly investigated. Since accurate determination of the optical functions is essential prerequisites for device simulations and gives the opportunity to improve material preparation, this necessitates the investigation of optical characteristics for $HfAlO_x$ thin films in the wide energy range. Thus, we need to understand the evolution of optical functions related to the annealing temperature. In this work, SE was used to extract the dependence of the optical functions on the postannealing temperature.

Figure 3 shows the SE experimental spectra and fitted theoretical curves for the as-deposited and annealed $HfAlO_x$ films at 600 °C. Compared to the as-deposited sample, the experimental spectra of the annealed samples demonstrate apparent change, indicating that annealing has magnificent effect on the optical properties. It can be seen that the fitted spectra reproduce almost identically the experimental spectra in the entire measured photon energy range. Therefore, it is verified that the four-layer-structured fitting models in SE analyses are adequate to describe the optical dispersion relation and the microstructure of the $HfAlO_x$ films. Based on

Downloaded 23 Jun 2010 to 61.190.88.137. Redistribution subject to AIP license or copyright; see http://jap.aip.org/jap/copyright.jsp

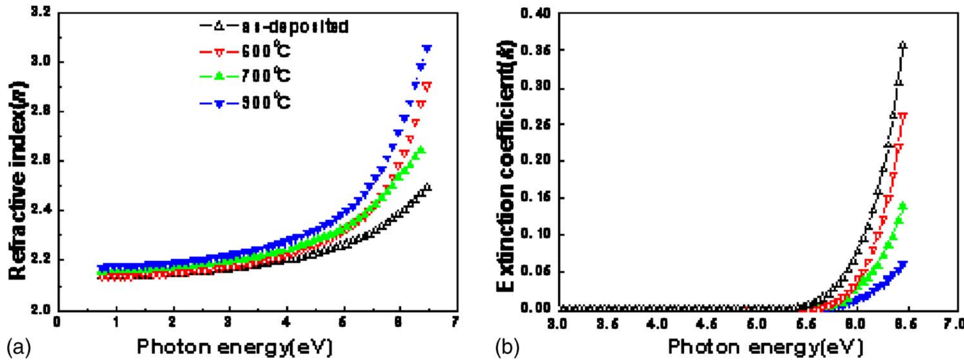

FIG. 4. (Color online) Refractive index spectra (a) and extinction coefficient spectra (b).

the simplified four-phase model, the film thickness is obtained as by-products. For the as-deposited, the thickness of the as-deposited sample is 7.25 nm. With the increase of annealing temperature, the thicknesses are found to be 7.05, 6.78, and 6.35 nm for the samples annealed at 600, 800, and 900 °C, respectively. Apparently, a decrease in the thickness of the annealed samples has been observed with increasing the annealing temperature. This decrease in the thickness can be attributed to the increasing packing density of the annealed $HfAlO_x$ films.

Figure 4 shows the refractive index n and extinction coefficient k calculated from the extracted best-fitted parameters. It has been indicated that there are large and discontinuous increases in values of refractive index, which can be correlated with the increase of packing density. The low values of packing density due to loose arrangement can attribute to the lower refractive index of the as-deposited thin films. Annealing accelerates the formation of more closely packed thin films, leading to a higher refractive index as well. Additionally, this result is also confirmed by the reduction of the fitted parameters for the film thickness. However, in the report of Thomas *et al.*, they observed a small decrease in density and a corresponding increase in thickness in $DyScO_\delta$ films with the annealing temperature up to 950 °C. They attributed it to the strong interdiffusion from Si into $DyScO_\delta$ and the formation of $Dy_xSc_ySi_zO_\delta$.[39] In our case, the formation of an interface layer consisting of silicates has been observed only in initial stage. With the increase of annealing temperature, the interdiffusion from Si substrate is not found, indicating that the silicate formation itself was well suppressed in the $HfAlO_x$ film. It can originate from the formation of dense SiO_x at the interfacial layer, which suppresses the interdiffusion and blocks the increase of the thickness. Shown in Fig. 4, it is worth noting that the nonzero extinction coefficient (k) at the high photon energy is related to the band-band transitions. Since k is related to the optical absorption, its value will have some change when the band gap energy changes. According to Fig. 4, it can be seen that there is a slight blueshift in the k tail edge after the additional high temperature annealing, indicating the change in the optical absorption properties.

Figure 5 presents the real (ε_1) and imaginary (ε_2) parts of the dielectric functions of the as-deposited and annealed samples. As seen in Fig. 5, it has been observed that annealing temperature has magnificent effect on the dielectric functions of the $HfAlO_x$ films. To estimate the bandgap values of the as-deposited and annealed $HfAlO_x$ films, the traditional Tauc plots of $[n(E)\alpha(E)E]^{1/2}$ versus photon energy E has been employed,[40] where $\alpha=4\pi k/\lambda$ is the absorption coefficient, λ is the light wavelength, and k is the extinct coefficient. Near the band edge of amorphous materials, Tauc plots display a linear relation with E; therefore, the bandgap can be extracted by extrapolating $[n(E)\alpha(E)E]^{1/2}$ to zero. From the plots in the inset of Fig. 5(b), the bandgap is estimated about 5.92 eV for the as deposited, which is higher than that of HfO_2. After annealing from 600 to 800 °C, there is a 0.04 eV shift of E_g toward higher bandgap. This increase can be explained by the phase separation contributed to crystallization. According to our previous result, pure HfO_2 crystallizes at temperature below 600 °C.[9,10] However, with Al_2O_3 incorporation into HfO_2, the crystallization temperature of the alloy increases by about 300 °C. After annealing at 900 °C, E_g increases to 6.13 eV. According to XRD measurement shown in the inset of Fig. 5(a), it is apparent that the film suffers phase separation into crystalline HfO_2 and

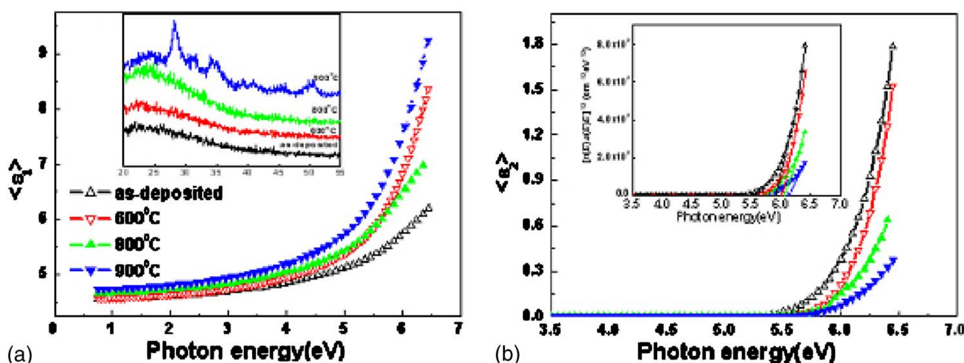

FIG. 5. (Color online) The real and imaginary parts of the pseudodielectric functions $\varepsilon=\varepsilon_1+\varepsilon_2$ of the as-deposited and annealed $HfAlO_x$ films at different temperatures. The insets are the annealing temperature dependence of the structure and optical bandgap energy. α and n is the absorption coefficient and refractive index calculated from the SE fitting, respectively.

Downloaded 23 Jun 2010 to 61.190.88.137. Redistribution subject to AIP license or copyright; see http://jap.aip.org/jap/copyright.jsp

amorphous Al_2O_3. It shows that, after annealing at 900 °C, the amorphous phase changes into a polycrystalline structure of HfO_2 reflecting the phase separation of the alloy into HfO_2 and Al_2O_3. As we know, E_g of Al_2O_3 is larger than that of HfO_2, and thus the increase of the bandgap related to annealing temperatures could be due to phase separation. Compared to pure Al_2O_3, a decreased band gap in Hf aluminate has been observed. It is believed that the intermixing of these two transition metal oxides, with Al_2O_3 having a larger bandgap, increases the separation of the oxygen 2*p* orbital valence band state and the antibonding *d* states intermixed of Hf and Al, and therefore results in a larger bandgap.[41] It indicates that the bandgap energy of Hf aluminate is mainly contributed to Hf 5*d* or O 2*p* states of HfO_2. According to the report of Lin *et al.*, the localized *d* states do not mix significantly with the extended *s*-like conduction band states of the Al_2O_3 host oxide. The electron states of Hf atoms substantially contributed to the conduction band (CB) edge.[33] According to our results, it can guess the localized *d* states below the CB minimum of Al_2O_3. After annealing at 900 °C, due to the mixed phase separation of $HfAlO_x$ film, the breaking of the Hf–Al–O bond will bring about the formation of dangling bonds, which distracts from the bandgap of the mixed oxide and make E_g differ from that of the as-deposited $HfAlO_x$.

IV. CONCLUSION

In summary, thermal stability and optical properties of ultrathin $HfAlO_x$ thin films on Si (100) substrates, grown by facing-target reactive sputtering, have been investigated as a function of annealing temperature. It has been found that the thermal stability is significantly enhanced and sustains up to the annealing temperature of 800 °C. Annealing at 900 °C accelerates the breaking of the Hf–Al–O bond and the phase separation of $HfAlO_x$. Additionally, the information of an interfacial Si–O–Si bond as the dominant reaction during the postannealing treatment has been determined. Temperature-independent optical functions are also determined by SE characterization. Increase in the refractive index and reduction in thickness have been observed as a function of annealing temperature, originating from the annealing-induced higher packing density. It has shown that the bandgap increases with annealing temperature, which can be due to the phase separation.

ACKNOWLEDGMENTS

This work was supported by the National Natural Science Foundation of China (Grant No. 10674138).

[1]G. D. Wilk, R. M. Wallace, and J. M. Anthony, J. Appl. Phys. **89**, 5243 (2001).
[2]A. I. Kingon, J.-P. Maria, and S. K. Streiffer, Nature (London) **406**, 1032 (2000).
[3]S. Miyazaki, J. Vac. Sci. Technol. B **19**, 2212 (2001).
[4]V. V. Afanas'ev, A. Stesmans, and W. Tsai, Appl. Phys. Lett. **82**, 245 (2003).
[5]C. T. Hsu, Y. K. Su, and M. Yokoyama, Jpn. J. Appl. Phys., Part 1 **31**, 2501 (1992).
[6]B. H. Lee, L. Kang, R. Nieh, W.-J. Qi, and J. C. Lee, Appl. Phys. Lett. **76**, 1926 (2000).
[7]K. J. Hubbard and D. G. Schlom, J. Mater. Res. **11**, 2757 (1996).
[8]W. Zhu, T. P. Ma, T. Tamagawa, Y. Di, J. Kim, R. Carruthers, M. Gibso, and T. Furukawa, Tech. Dig. - Int. Electron Devices Meet. **2001**, 20.4.1.
[9]G. He, Q. Fang, M. Liu, L. Q. Zhu, and L. D. Zhang, J. Cryst. Growth **268**, 155 (2004).
[10]G. He, M. Liu, L. Q. Zhu, M. Chang, Q. Fang, and L. D. Zhang, Surf. Sci. **576**, 67 (2005).
[11]G. D. Wilk, R. M. Wallace, and J. M. Anthony, J. Appl. Phys. **87**, 484 (2000).
[12]A. Kumar, D. Rajdev, and D. L. Douglass, J. Am. Chem. Soc. **55**, 439 (1972).
[13]C. S. Kang, H.-J. Cho, K. Onishi, R. Choi, Y. H. Kim, R. Nieh, J. Han, S. Krishnan, A. Shahriar, and J. C. Lee, Tech. Dig. - Int. Electron Devices Meet. **2002**, 865.
[14]C. H. Choi, S. J. Rhee, T. S. Jeon, N. Lu, J. H. Sim, R. Clark, M. Niwa, and D. L. Kwong, Tech. Dig. - Int. Electron Devices Meet. **2002**, 857.
[15]V. Mikhelashvili, R. Brener, O. Kreinin, B. Meyler, J. Shneider, and G. Eisenstein, Appl. Phys. Lett. **85**, 5950 (2004).
[16]H. Y. Yu, N. Wu, M. F. Li, C. X. Zhu, B. J. Cho, D. L. Kwang, C.-L. Tung, J. S. Pan, J. W. Chai, W. D. Wang, D. Z. Chi, C. H. Ang, J. Z. Chi, and S. Ramanathan, Appl. Phys. Lett. **81**, 3618 (2002).
[17]M.-H. Cho, Y. S. Roh, C. N. Whang, K. Jeong, H. J. Choi, S. W. Nam, D.-H. Ko, J. H. Lee, N. I. Lee, and K. Fujihara, Appl. Phys. Lett. **81**, 1071 (2002).
[18]H. Y. Yu, M. F. Li, B. J. Cho, C. C. Yeo, M. S Joo, D. L. Kwang, J. S. Pan, C. H. Ang, J. Z. Zheng, and S. Ramanathan, Appl. Phys. Lett. **81**, 376 (2002).
[19]S. J. Ding, C. X. Zhu, M. F. Li, and D. W. Zhang, Appl. Phys. Lett. **87**, 053501 (2005).
[20]M. Liu, G. He, L. Q. Zhu, Q. Fang, G. H. Li, L. D. Zhang, Appl. Surf. Sci. **252**, 6206 (2006).
[21]M. S. Joo, B. J. Cho, C. C. Yeo, D. S. Chan, S. J. Whoang, S. Mathew, L. K. Bera, N. Balasubramanian, and D. Kwong, IEEE Trans. Electron Devices **50**, 2088 (2003).
[22]M. H. Cho, H. S. Chang, Y. J. Cho, D. W. Moon, K. H. Min, R. Sinclair, S. K. Kang, D. H. Ko, J. H. Lee, J. H. Gu, and N. I. Lee, Appl. Phys. Lett. **84**, 571 (2004).
[23]K. Kukli, M. Ritala, T. Sajavaara, J. Kemonen, and M. Leskla, Thin Solid Films **416**, 72 (2002).
[24]M. Takahashi and S. Sakai, Jpn. J. Appl. Phys., Part 2 **44**, L800 (2005).
[25]S. Sakai, R. Ilangovan, and M. Takahashi, Jpn. J. Appl. Phys., Part 1 **43**, 7876 (2004).
[26]G. He, L. D. Zhang, G. H. Li, M. Liu, L. Q. Zhu, S. S. Pan, and Q. Fang, Appl. Phys. Lett. **86**, 232901 (2005).
[27]G. He, J. X. Zhang, L. Q. Zhu, M. Liu, Q. Fang, and L. D. Zhang, Nanotechnology **16**, 1641 (2005).
[28]M. Liu, Q. Fang, G. He, L. Li, L. Q. Zhu, G. H. Li, and L. D. Zhang, Appl. Phys. Lett. **86**, 232901 (2005).
[29]W. Kern and D. A. Poutinen, RCA Rev. **31**, 187 (1970).
[30]C. M. Herzinger, B. Johs, W. A. McGahan, J. A. Woollam, and W. Paulson, J. Appl. Phys. **83**, 3323 (1998).
[31]E. D. Palik, *Handbook of Optical Constants of Solids* (Academic, Orlando, FL, 1985).
[32]D. A. G. Bruggemann, Ann. Phys. **24**, 636 (1935).
[33]H. Jin, S. K. Oh, H. J. Kang, S. W. Lee, Y. S. Lee, and M.-H. Cho, Appl. Phys. Lett. **87**, 212902 (2005).
[34]J. Zhu, Z. G. Liu, and Y. R. Li, J. Phys. D **38**, 446 (2005).
[35]T. S. Jeon, J. M. White, and D. L. Kwong, Appl. Phys. Lett. **78**, 368 (2001).
[36]H. Y. Yu, N. Wu, M. F. Li, C. X. Zhu, B. J. Cho, D.-L. Kwong, C. H. Tung, J. S. Pan, J. W. Chai, W. D. Wang, D. Z. Chi, C. H. Ang, J. Z. Zheng, and S. Ramanathan, Appl. Phys. Lett. **81**, 3618 (2002).
[37]S. Iwata and A. Ishizaka, J. Appl. Phys. **79**, 6653 (1996).
[38]G. He, Q. Fang, and L. D. Zhang, J. Appl. Phys. **100**, 083517 (2006).
[39]R. Thomas, P. Ehrhart, M. Luysberg, M. Boese, R. Waser, M. Roeckerath, E. Rije, J. Schubert, S. V. Elshocht, and M. Caymax, Appl. Phys. Lett. **81**, 3618 (2002).
[40]J. Tauc, R. Grigorovici, and A. Vancu, Phys. Status Solidi **15**, 627 (1966).
[41]G. Lukovsky, J. L. Whitten, and Y. Zhang, Microelectron. Eng. **59**, 329 (2001).

Downloaded 23 Jun 2010 to 61.190.88.137. Redistribution subject to AIP license or copyright; see http://jap.aip.org/jap/copyright.jsp